

Original Article



MicroRNA-21 Inhibition Suppresses Alveolar M2 Macrophages in an Ovalbumin-Induced Allergic Asthma Mice Model

Hwa Young Lee , Jung Hur , Ji Young Kang , Chin Kook Rhee ,
Sook Young Lee

Division of Allergy, Pulmonary and Critical Care Medicine, Department of Internal Medicine, Seoul St. Mary's Hospital, College of Medicine, The Catholic University of Korea, Seoul, Korea

OPEN ACCESS

Received: Apr 30, 2020

Revised: Aug 12, 2020

Accepted: Aug 14, 2020

Correspondence to

Sook Young Lee, MD, PhD

Division of Allergy, Pulmonary and Critical Care Medicine, Department of Internal Medicine, Seoul St. Mary's Hospital, College of Medicine, The Catholic University of Korea, 222 Banpo-daero, Seocho-gu, Seoul 06591, Korea.

Tel: +82-2-2258-6062

Fax: +82-2-569-2158

E-mail: sooklee@catholic.ac.kr

Copyright © 2021 The Korean Academy of Asthma, Allergy and Clinical Immunology · The Korean Academy of Pediatric Allergy and Respiratory Disease

This is an Open Access article distributed under the terms of the Creative Commons Attribution Non-Commercial License (<https://creativecommons.org/licenses/by-nc/4.0/>) which permits unrestricted non-commercial use, distribution, and reproduction in any medium, provided the original work is properly cited.

ORCID iDs

Hwa Young Lee

<https://orcid.org/0000-0002-1582-2256>

Jung Hur

<https://orcid.org/0000-0002-6098-2224>

Ji Young Kang

<https://orcid.org/0000-0003-4942-013X>

Chin Kook Rhee

<https://orcid.org/0000-0003-4533-7937>

Sook Young Lee

<https://orcid.org/0000-0002-3346-3664>

ABSTRACT

Purpose: MicroRNA-21 (miR-21) influences the Th2 immune pathway by suppressing the expressions of interleukin (IL)-12 and interferon (IFN)- γ . The effects of miR-21 suppression on alveolar macrophage polarization and airway inflammation are not known.

Methods: BALB/c and miR-21 knockout (KO) mice were sensitized and challenged with ovalbumin (OVA). The anti-miR-21 antagomir was administered to BALB/c mice by intranasal inhalation from the day of OVA sensitization. Changes in cell counts, cytokine levels in bronchoalveolar lavage fluid (BALF), and airway hyperresponsiveness (AHR) were examined. Total, M1, and M2 macrophages were examined in the lung tissues by immunohistochemistry (IHC). M2 macrophages from the OVA mice lung were inhaled into the anti-miR-21 antagomir-treated asthmatic mice. Moreover, the polarization of M0 to M2 macrophages upon IL-4 stimulation was analyzed after anti-miR-21 antagomir transfection.

Results: The miR-21 KO mice showed decreases in AHR, total cell and eosinophil counts in BALF, and in the levels of IL-4, IL-5, IL-10, and IL-13. Expression of IL-12 and IFN- γ were increased in the miR-21 KO mice. Peribronchial inflammation and goblet cell dysplasia were significantly decreased in the lung tissues of miR-21 KO OVA mice compared to the wild type OVA mice. IHC for M1, M2, and total macrophage in the lung tissues showed that miR-21 inhalation suppressed alveolar M2 macrophages in KO mice. M2 macrophage inhalation restored AHR and eosinophilic airway inflammation in the miR-21 antagomir-treated mice. Moreover, anti-miR-21 antagomir transfection decreased the expression of M2 markers and increased the expression of M1 markers in M0 macrophages after IL-4 stimulation.

Conclusions: The results suggest that miR-21 antagonism could suppress alveolar M2 macrophage polarization, decreasing not only the Th2 eosinophilic airway inflammation but also AHR and airway remodeling process.

Keywords: Asthma; microRNAs; macrophages, miR-21 antagomir, AHR

INTRODUCTION

Bronchial asthma is a chronic airway disease characterized by airway inflammation and airway remodeling. Airway inflammation is mediated by not only epithelial cells but also by immune cells such as dendritic cells, T lymphocytes, innate lymphoid cells, and

Disclosure

There are no financial or other issues that might lead to conflict of interest.

macrophages.^{1,2} Traditional pathophysiology of allergic asthma is explained as the Th2 high pathway; however, the roles of pulmonary macrophages in mediating interactions with T cells are emerging.

Macrophages are innate immune cells that mediate initial response to immune stimuli and are involved in the development of innate and adaptive immune responses.³ Depending on the micro-environmental stimuli, macrophages may polarize classic pro-inflammatory M1 or alternative M2 macrophages.⁴ In bronchial asthma, macrophages play different roles in phagocytosis, efferocytosis, production of inflammatory mediators, and polarizations.³ Previous literatures have reported increased levels of alveolar macrophages and M2 phenotypes in bronchoalveolar lavage fluid (BALF)⁵ and airway wall tissues⁶ in patients with bronchial asthma. It is well known that activation of M1/M2 macrophages is associated with changes in the level of cytokines and interferon (IFN)- γ in M1 macrophages, and interleukin (IL)-4 and IL-13 in the M2 phenotype, which are both linked with Th1 and Th2 immune responses.⁷ However, factors affecting alveolar macrophage polarization in bronchial asthma are under-investigated.

Micro-RNAs (miRNAs) are single-stranded RNA molecules that modulate protein expression via post-transcriptional silencing.⁸ MiR-21 is one of the important mediators of bronchial asthma, expressed principally in macrophages and dendritic cells.^{9,12} By targeting the 3'UTR of IL-12p35 protein, miR-21 regulates immune polarization, limits the production of Th1 cytokines, and increases the Th2 immune pathway.¹³ In a previous study, intranasal administration of miR-21 antagomir successfully decreased airway eosinophilic inflammation, AHR, and generation of splenocyte Th2 cells by decreasing the expression of signal transducer and activator of transcription (STAT) 6 phosphorylation.¹⁴

To examine the role of miR-21 in alveolar macrophage polarization and Th2 immune pathway in bronchial asthma, we explored the effect of miR-21 deficiencies in eosinophilic airway inflammation, AHR, and lung tissues with ovalbumin (OVA) sensitization and challenge in miR-21^{-/-} mice. To examine M1 and M2 macrophage polarization, immunohistochemistry (IHC) stain for total macrophage (CD68), M1 macrophage (IFN regulatory factor 5 [IRF-5]), and M2 macrophage (YM-1) were done in lung tissues. M2 macrophages isolated from OVA asthmatic mice were inhaled into anti-miR-21 antagomir-treated mice to determine if these effects of miR-21 deficiency were mediated by M2 macrophages. Moreover, an *in vitro* study was performed employing M0 macrophages (RAW264.7) by transfection with anti-miR-21 antagomir before IL-4 stimulation. We measured the expression of each biomarker for M1 and M2 macrophages by quantitative real-time reverse-transcription polymerase chain reaction (qRT-PCR) and western blot analysis.

MATERIALS AND METHODS

Animals and experimental design

MiR-21 knockout (KO) female mice (129S6-Mir21 $\alpha^{tm1Yoli/J}$); stock No:016856, miR-21 null) were purchased from Jackson Laboratories (Bar Harbor, ME, USA) and control wild type (WT) C57/BL6 mice were from Dae-Han Experimental Animal Center (Daejeon, Korea). Six-week-old female BALB/c mice (Dae-Han Experimental Animal Center) were used for the generation of an miR-21 antagomir inhalation model.

Mice were housed in a controlled environment with a 12-hour light/dark cycle with free access to food and water, and were maintained on an OVA-free diet. All procedures of animal research were performed following the Laboratory Animals Welfare Act, the Guide for the Care and Use of Laboratory Animals and the Guidelines and Policies for Rodent experiment provided by the Institutional Animal Care and Use Committee in School of Medicine, The Catholic University of Korea (approval No. CUMC-2015-0180-03).

Mice were assigned to 1 of the 4 groups: 1) control WT; 2) WT OVA challenge; 3) miR-21 KO control; and 4) miR-21 KO OVA challenge. For miR-21 antagomir inhalation, the other 4 groups: 1) control; 2) OVA challenge; 3) OVA challenge with intranasal inhalation of scrambled RNA; and 4) OVA challenge with intranasal inhalation of anti-miR-21 antagomir, were used.

Sensitization and antigen challenge protocol

Mice were sensitized and challenged with OVA as previously described.¹⁵ Sensitization was done by subcutaneous injection of OVA (Sigma-Aldrich, St. Louis, MO, USA) adsorbed to 1 mg of aluminum hydroxide (Aldrich, Milwaukee, WI, USA) in 200 μ L of normal saline. After sensitization on days 1 and 8, challenges were done by intranasal inhalation of OVA (20 ng/50 μ L in phosphate-buffered saline [PBS]) on days 21, 23, 25, and 28 under isoflurane (Vedco, St. Joseph, MO, USA) anesthesia. The control groups were treated in the same way with PBS without OVA. Mice were sacrificed 24 hours after the final OVA challenge after measuring AHR.

Antagomir administration

Commercially available anti-miR-21 antagomir was purchased for the animal study from Ambion[®] (Austin, TX, USA) and anti-scrambled RNA from Cosmogenetech (Shanghai GenePharma. Ltd, Shanghai, China). Antagomir sequence was as follows: 5'-mA*mC*mG mGmCmA mAmCmA mCmCmA mGmUmC mGmAmU mGmGmG mC*mU*mG* mU*-3'-chol; where m denotes 2'-O-Methyl-modified phosphoramidities, * denotes phosphorothioate linkages, and chol denotes hydroxyprolinol-linked cholesterol. We intranasally administered 50 μ g of anti-miR-21 or anti-scrambled RNA mixed in 50 μ L of sterile saline 30 minutes before the OVA challenge on the day of sensitization (days 1 and 8) and then once a day from the day of the challenge until sacrifice (days 20, 21, 22, 23, 24, and 27).

Measurement of AHR and bronchoalveolar lavage (BAL)

AHR to methacholine (Mch; Sigma-Aldrich) was measured after the final OVA challenge using the flexiVent system (SCIREQ, Montreal, Quebec, Canada).¹⁶ BAL was performed immediately after the measurement of AHR. Initially, the mice were anesthetized with an intraperitoneal injection of rompun and zoletil mixture (1:4). Subsequently, the trachea was exposed and cannulated to a computer-controlled small-animal ventilator and ventilated with a tidal volume of 10 mg/kg at a frequency of 150 breaths/min and a positive end-expiratory pressure of 2cmH₂O to achieve a mean lung volume close to that during spontaneous breathing. Each mouse was exposed to PBS and then to increasing concentrations of Mch in PBS (6.25, 12.5, 25, and 50 mg/mL). The peak airway responses to the inhaled Mch were recorded. BALF was withdrawn after instillation of 1 mL of sterile PBS through the trachea into the lung. After counting of the number of total cells in BALF using a hemacytometer, BALF cytopsin (7 minutes at 20,000 rpm) slides were prepared and stained with Diff-Quick (Sysmax, Kobe, Japan). The percentages of macrophages, eosinophils, lymphocytes, and neutrophils were obtained by counting 400 leukocytes on the randomly selected area of the slide using light microscopy. The supernatant was stored at -70°C.

Enzyme-linked immunosorbent assay (ELISA)

The levels of IL-4, IL-5, IL-10, IL-13, and IFN- γ were measured in the supernatant of BALF and IL-12p70 in lung tissues with an ELISA kit (R&D Systems, Minneapolis, MN, USA). The protocol was followed according to the manufacturer's instructions. The sensitivities of the IL assays were 2, 7, 5.22, 1.5, 2, and 2.5 pg/mL, respectively. Reactions were read using an ELISA plate reader at 450 nm.

Lung tissue histopathology

After obtaining BALF, the lungs were inflated, fixed in 4% paraformaldehyde for 24 hours, and embedded in paraffin wax. Sections were cut at 4- μ m thickness using a microtome and stained with hematoxylin and eosin (H&E) using standard techniques for assessing histological changes. The degree of perivascular or peribronchial inflammation was assessed as previously described.¹⁷ The following 5-point scoring system (grade 0–4) was used: no inflammation (grade 0); occasional cuffing with inflammatory cells (grade 1); and most bronchi or vessels surrounded by a thin layer (grade 2), moderate layer (grade 3), or thick layer (grade 4) of inflammatory cells. For periodic acid-Schiff (PAS) staining, the paraffin-embedded tissues were sectioned at 5–6 μ m and stained with PAS to identify goblet cells in the epithelium. To quantify goblet cell hyperplasia, pathological changes were evaluated according to the method described by Padrid *et al.*¹⁸ The percentage of goblet cells in the epithelium scored as follows: no goblet cells = 0, < 25% = 1, 25%–50% = 2, 51%–75% = 3, and > 75% = 4. α -smooth muscle actin (α -SMA) was immunohistochemically detected as previously described.¹⁹ The area in each paraffin-embedded lung immunostained by α -SMA was outlined and quantified using a light microscope attached to an image analysis system (BX50; Olympus, Tokyo, Japan). The results were expressed as the immunostained area of the bronchiolar basement membrane (internal diameter 150–200 μ m, internal diameter). At least 10 bronchioles were counted in each slide.

Immunohistochemical staining of macrophages

Six micrometer-thick sections were stained for the determination of total macrophages (goat α CD68; Santa Cruz Biotechnology, Santa Cruz, CA, USA). M2 macrophages were determined by staining for YM1 (goat α YM1/Chitinase 3-like 3; R&D Systems, Oxon, UK) and M1 macrophages for IRF-5 (rabbit α IRF-5; Santa Cruz Biotechnology) using the standard immunohistochemical procedure. Immunoreactivity was detected by sequential incubations of the lung section with a biotinylated secondary antibody, followed by peroxidase reagent (Vector Lab, Burlingame, CA, USA) and diaminobenzidine chromogen (Invitrogen, Carlsbad, CA, USA). The average stained area was quantified on the 8 to 10 images of mouse ($n = 3$ –8) utilizing Image J software (National Institutes of Health, Bethesda, MD, USA). The number of cells was expressed per mm² of tissue.

Cell culture, transfection, and signal activation

The murine macrophage cell line RAW 264.7 (American Type Culture Collection, Manassas, VA, USA) was cultured in DMEM medium (Hyclone, Logan, UT, USA) supplemented with 10% fetal bovine serum as well as 1% penicillin and streptomycin solution (10,000 units/mL penicillin and 10 mg/mL streptomycin). Cells were incubated in a humidified incubator at 37°C under an atmosphere of 5% CO₂ and were split regularly before they attained approximately 80% confluence.

We used the mirVena™ miR-21 inhibitor to inhibit the expression of miR-21 in RAW264.7 cells. The mirVena™ miRNA-negative inhibitor was used as the negative control (NC).

RAW264.7 cells were grown on 6-well plates overnight. Cells at 60%–70% confluence were transfected with 30 pmole of the miR-21 inhibitor or miR-21-negative inhibitor using RNAiMax (Invitrogen).

After 72 hours of transfection, cells were directly treated with 10 ng/mL (20 ng/mL for western blot analysis of IRF-5) of recombinant mouse IL-4 (rmIL-4, R&D systems) for 18 hours. Experiments were performed in triplicate.

Replacement of M2 macrophages in mice administered with an miR-21 inhibitor

M2 macrophages were isolated from the OVA asthmatic mice lung (n = 5) after the last OVA challenge. The lungs were digested with 1 mg/mL collagenase IV (Sigma), 1 mg/mL deoxyribonuclease I (Sigma), and red blood cells were lysed. Lung single-cell suspensions were blocked with anti-CD16/CD32 (eBioscience, San Diego, CA, USA) before staining. For M2 macrophage sorting, cells were stained with anti-CD45, anti-F4/80, and anti-CD206 antibodies (eBioscience) for 1 hour and then sorted by fluorescence-activated cell sorting (FACS) using a FACSaria Fusion (BD Biosciences, Franklin Lakes, NJ, USA). M2 macrophages were defined as CD45⁺F4/80⁺CD206⁺ cells (**Supplementary Fig. S1A**).

We intranasally administered 50 µg of mirVena™ miR-21 inhibitor (Ambion; Applied Biosystems, Foster City, CA, USA) mixed in 50 µL of PBS 30 minutes before the OVA challenge 3 times a week during challenge until sacrifice (days 21, 23, 25 and 28). Isolated M2 macrophages (1 × 10⁵ cells/50µL in PBS) were administered intranasally on the day of last OVA challenge (**Supplementary Fig. S1B**).

Real-time PCR

For qRT-PCR analysis of IL-1β, IL-6, C-type mannose receptor 1 (MRC1), and arginase 1 (ARG1) gene expressions, total RNA was isolated from lung homogenates using TRIzol reagent™ (Invitrogen) according to the manufacturer's protocol. The total RNA (1 µg) was reverse-transcribed and qRT-PCR was performed using a CFX96 Real-Time PCR Detection System (Bio-Rad Laboratories, Hercules, CA, USA). Amplification was done using the selective primers described in **Table 1**, and iQ SYBR gene expression assay (Bio-Rad Laboratories), according to the manufacturer's instructions.

Western blot analysis

Total protein was isolated from the lungs by homogenization in radioimmunoprecipitation assay cell lysis buffer containing a mixture of protease inhibitor and phosphatase inhibitor

Table 1. Sequence of primers used in this work

Primer name	F/R	Sequence (5' to 3')
GAPDH_Ms	F	AGA ACA TCA TCC CTG CAT CC
	R	CAC ATT GGG GGT AGG AAC AC
IL-1β_Ms	F	AAC CTC ACC TAC AGG GCG TTC A
	R	TGT AAT GAA AGA CGG CAG GCA GCA GCG
IL-6_Ms	F	CCA CTT CAC AAG TCG GAG GCT TA
	R	AGT GCA TCA TCG TTG TTC ATA C
MRC1_Ms	F	CAT GAG GCT TCT CCT GCT TCT
	R	TTG CCG TCT GAA CTG AG TGG
ARG1_Ms	F	CTC CAA GCC AAA GTC CTT AGA G
	R	AGG AGC TGT CAT TAG GGA CAT C

GAPDH, glyceraldehyde 3-phosphate dehydrogenase; IL, interleukin; MRC1, mannose receptor 1; ARG1, arginase 1; F, forward; R, reverse; Ms, mouse.

(GenDEPOT, Barker, TX, USA), followed by centrifugation 13,000 rpm for 30 minutes at 4°C. Protein concentration was quantified using the BCA assay. The equal amount of sample protein (70 µg) was separated by sodium dodecyl sulfate-polyacrylamide gel electrophoresis and transferred to polyvinylidene difluoride membranes (Amersham Pharmacia Biotech, Little Chalfont, UK). The membranes were blocked with 5% skim milk (Difco/Becton Dickinson, Atlanta, GA, USA) for 1 hour at room temperature, followed by incubation with a 1:100 dilution of anti-IRF5 (rabbit α -IRF5, Santa Cruz Biotechnology) in 5% skim milk in Tris-buffered saline containing 0.1% Tween 20 overnight at 4°C. After incubation, the blot was washed and incubated with a 1:10,000 dilution of anti-rabbit-immunoglobulin G, horseradish peroxidase-linked secondary antibody (Jackson ImmunoResearch, West Grove, PA, USA) for 1 hour at room temperature. After washing, the protein bands were visualized by enhanced chemiluminescence using a RAS 3000 Image Analysis System (Fujifilm, Tokyo, Japan).

Statistical analysis

The data were subjected to 1-way analysis of variance followed by Dunnett's multiple range test using Graph-Pad Prism version 5.00 for Windows (GraphPad Software, San Diego, CA, USA). All data are expressed as means \pm standard error of the mean and in all cases, $P < 0.05$ was considered statistically significant.

RESULTS

MiR-21 KO suppresses AHR and inflammation in the OVA-sensitized and -challenged mouse model

Fig. 1A demonstrates changes in AHR in response to increasing doses of Mch in the mouse groups. OVA sensitization and challenge significantly increased AHR in the WT mice compared to the WT control ($P < 0.001$). In miR-21 KO mice, AHR decreased significantly after OVA sensitization and challenge compared to the WT OVA mice ($P < 0.001$). **Fig. 1B** presents the total and differential counts of airway inflammatory cells in BALF. OVA sensitization and challenge significantly increased total and eosinophil cell count ($P < 0.001$) compared to the control WT mice. On the contrary, the total and eosinophil cell count were suppressed in the miR-21 KO mice group ($P < 0.001$).

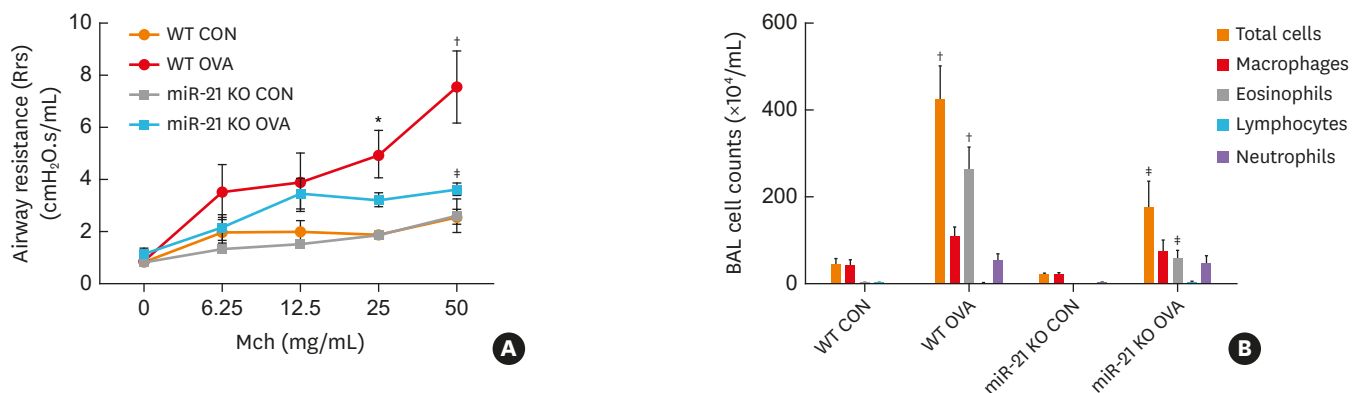


Fig. 1. Effect of miR-21 KO on AHR to Mch and total, differential cell counts in BAL fluid. AHR was measured 24 hours after the final OVA challenge using a flexiVent system in which the mice were exposed to increasing concentrations of Mch (6.25–50 mg/mL) (A). Mice were sacrificed 24 hours after the final OVA challenge and the BAL cells were isolated (B). The values are expressed as the mean \pm standard error of the mean ($n = 5-8$ /group).

AHR, airway hyperresponsiveness; Rrs, respiratory system resistance; WT, wild type; CON, control; miR-21, microRNA-21; KO, knock-out; OVA, ovalbumin; BAL, bronchoalveolar lavage; Mch, methacholine.

* $P < 0.01$, † $P < 0.001$ compared to the CON group; * $P < 0.001$ compared to the WT OVA group.

MiR-21 KO significantly decreases the infiltration of peribronchial airway inflammatory cells, goblet cell hyperplasia and α -SMA in mice lung tissues

H&E stain of the lung tissues showed that peribronchial airway infiltration of inflammatory cells was significantly increased in the WT asthmatic mice compared to the WT control mice and decreased in the miR-21 KO group (**Fig. 2A**). **Fig. 2B** presents increased inflammatory scores in the WT OVA mice and decreased scores in the miR-21 KO OVA mice compared to the WT asthma group ($P < 0.001$).

Fig. 2C reveals an increase in bronchial goblet cell proliferation in the WT OVA mice compared to the WT control mice and suppression in the miR-21 KO mice compared to the WT OVA group. **Fig. 2D** quantifies the PAS point scores with a comparative analysis between the groups. The PAS scores were significantly decreased in the miR-21 KO OVA mice compared to the WT OVA group.

Fig. 2E and F shows an increase in the lung tissue α -SMA stained area in the WT OVA mice compared to the WT control mice. In the miR-21 KO mice, α -SMA area was significantly decreased compared to the WT OVA mice.

MiR-21 efficiently decreases the expression of Th2 cytokines and increased Th1 cytokines

Fig. 3 shows the results of ELISA tests performed in BALF and lung tissues. Th2 cytokines, such as IL-4, IL-5, and IL-13, were increased in the WT OVA mice and significantly decreased in the miR-21 KO OVA mice. On the contrary, Th1 cytokine IFN- γ and IL-12p70 were increased in the miR-21 KO OVA mice compared to the WT OVA group. The expression of IL-10 was decreased in the miR-21 KO OVA mice compared to the WT OVA mice.

MiR-21 KO or miR-21 antagomir inhalation decreases M2 macrophages in lung tissues of OVA mice

Lung tissues from the miR-21 KO and WT mice were IHC-stained for the analysis of macrophage markers. **Figs. 4** and **5** show the results of IHC staining. YM-1-positive cells were increased in the WT OVA mice and significantly decreased in the lung tissues of miR-21 KO OVA (**Fig. 4F**) and miR-21 antagomir-inhaled OVA mice (**Fig. 5F**). No changes in IRF-5-stained cells were observed in the miR-21 KO mice compared to the WT OVA mice (**Fig. 4D**); however, the miR-21 antagomir inhaled mice demonstrated a statistically significant increase in IRF-5 stained cells compared to the scrambled micro-RNA-inhaled OVA mice (**Fig. 5D**). Cell counts of total macrophages in the lung tissues were slightly increased in the miR-21 KO OVA mice compared to the WT OVA mice and the miR-21 KO control mice; however, there was no statistically significant difference (**Fig. 4B**). In the lung tissues of miR-21 antagomir or control scrambled RNA-inhaled mice, OVA sensitization and challenge increased total macrophage cell counts compared to the control mice (**Fig. 5B**). MiR-21 antagomir inhalation led to a slight increase in total macrophage cells compared to the scrambled RNA-inhaled OVA group without any statistical significance (**Fig. 5B**).

Biomarkers for M1 and M2 macrophages are altered in miR-21 antagomir transfected macrophage cell lines after rmIL-4 stimulation

The *In vitro* study was performed to explore the effect of miR-21 on M1 and M2 polarization from M0 macrophages. **Fig. 6** shows the qRT-PCR results and **Fig. 7** demonstrates the results of western blot analysis. IL-1 β and IL-6 were used as M1 biomarkers and MRC1 and ARG1 were used as biomarkers for M2. After rmIL-4 stimulation, control scrambled RNA transfected

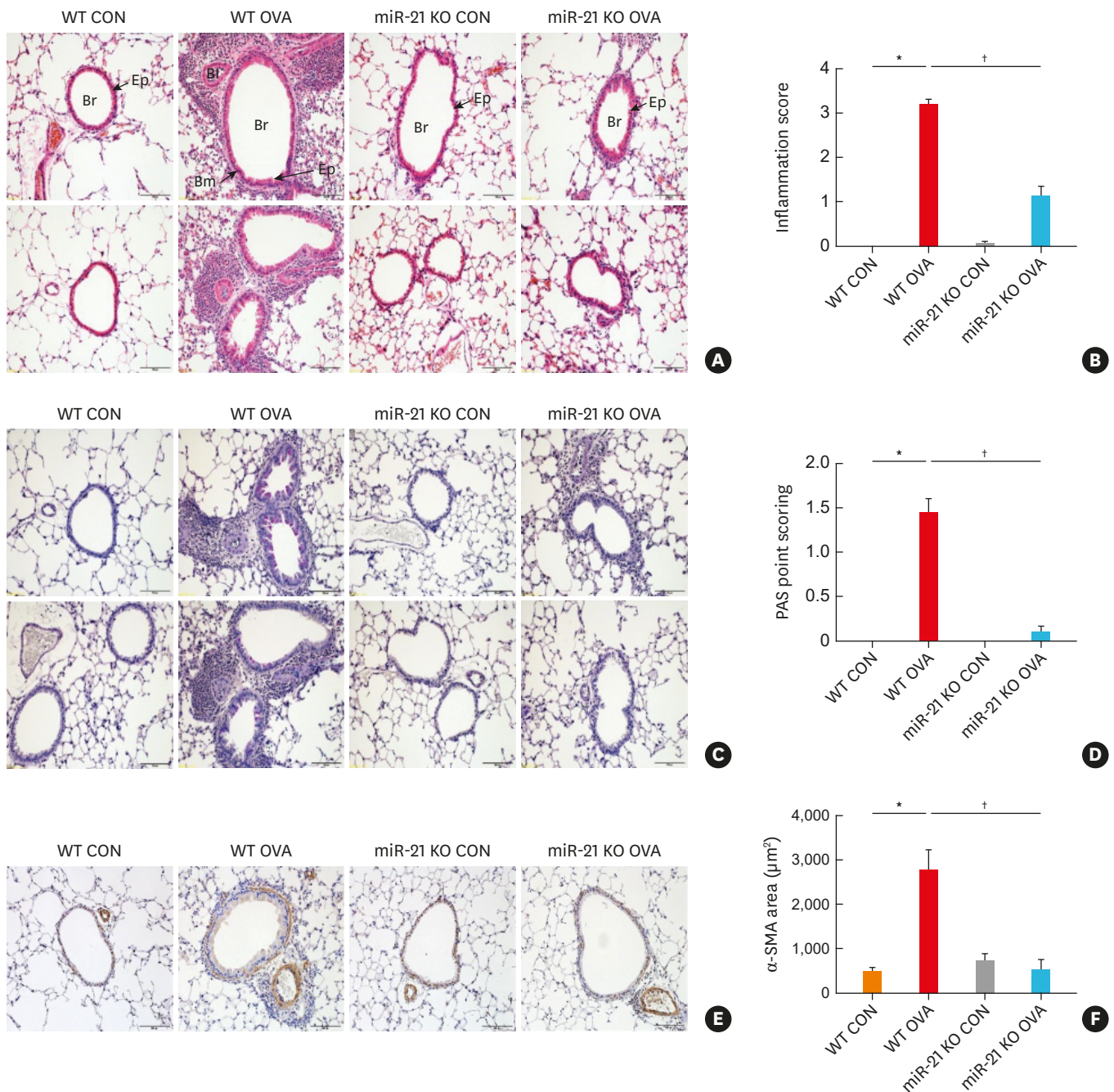


Fig. 2. Effect of miR-21 KO on lung histopathology, inflammation scores, goblet cell hyperplasia and α -SMA area. Representative photomicrographs of hematoxylin and eosin (A) stained lung sections from mice of the different treatment groups are shown ($\times 200$). Quantification of inflammation by point scoring (B). PAS (C) stained lung section from mice ($\times 200$) and quantification of point scores (D). Peribronchial α -SMA (E) was immunostained and stained area was quantified using an image analysis system (F). The results are expressed as the immunostained area per unit basement membrane length (μm). The values are expressed as the mean \pm standard error of the mean ($n = 5-8/\text{group}$).

WT, wild type; CON, control; OVA, ovalbumin; α -SMA, α -smooth muscle actin; miR-21, microRNA-21; KO, knock-out; PAS, periodic acid-Schiff; Br, bronchus; Bm, basement membrane; Eo, eosinophil; Ep, epithelium; Bv, blood vessel.

* $P < 0.001$ compared to the CON group; † $P < 0.001$ compared to the WT OVA group.

cells (NC) showed decreased the expression of IL-1 β and IL-6 ($P < 0.01$) compared to non-stimulated cells. However, anti-miR-21 transfected macrophage cells showed increased expression of IL-1 β and IL-6 ($P < 0.05$) after rmIL-4 exposure (Fig. 6A) compared to NC.

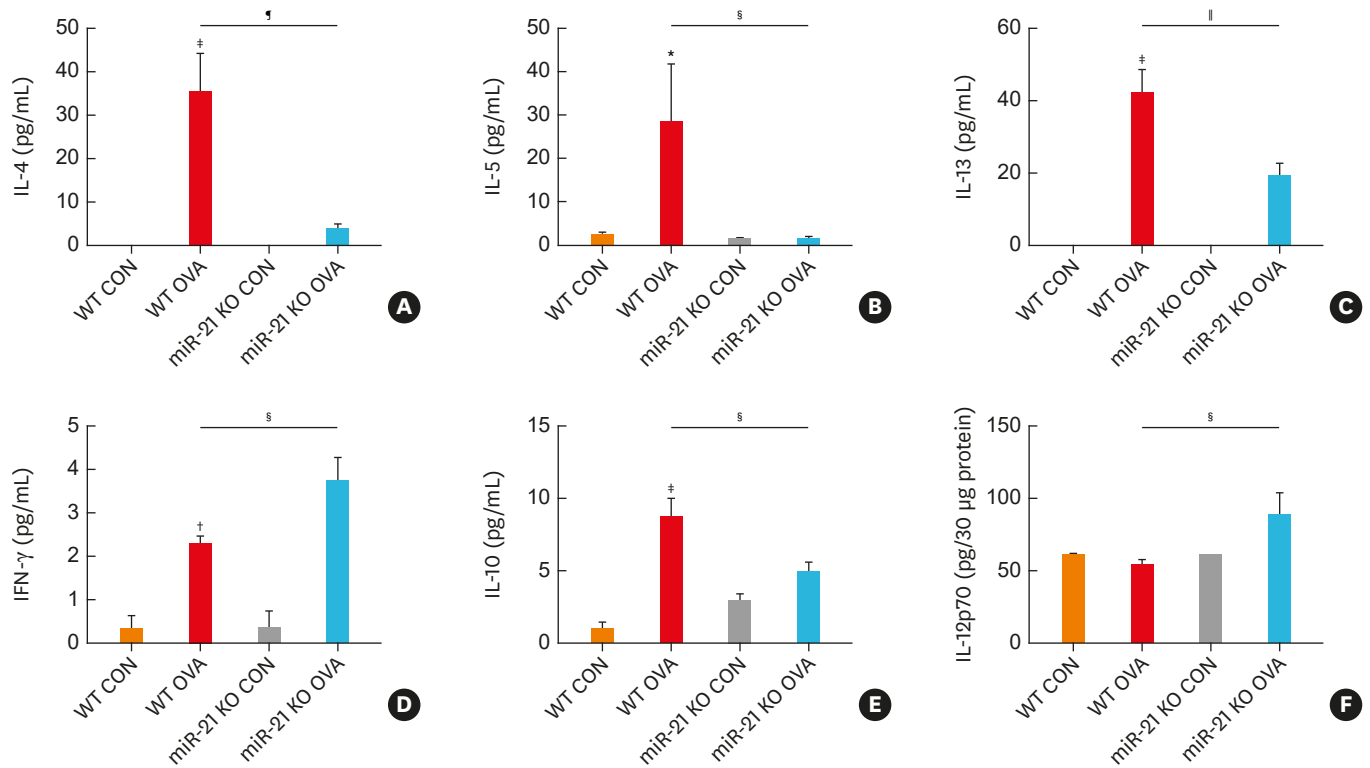


Fig. 3. Effect of miR-21 KO on signaling-related cytokine levels in BALF. The concentrations of IL-4 (A), IL-5 (B), IL-13 (C), IFN- γ (D), IL-10 (E) and IL-12p70 (F) in BALF were measured by enzyme-linked immunosorbent assays.

IL, interleukin; WT, wild type; CON, control; OVA, ovalbumin; KO, knock-out; miR-21, microRNA-21; IFN, interferon.

* $P < 0.05$, † $P < 0.01$, ‡ $P < 0.001$ compared to the CON group; § $P < 0.05$, ¶ $P < 0.01$, and ¶ $P < 0.001$ compared to the WT OVA group.

MRC1 and *ARG1* genes were significantly increased in both scrambled RNA and anti-miR-21 antagomir transfected cells after rmIL-4 stimulation. MiR-21 antagomir transfection suppressed expressions of *MRC1* ($P < 0.01$) and *ARG1* ($P < 0.001$) increased by rmIL-4 exposure in MO macrophage cells (Fig. 6B). Fig. 7 shows the western blot analysis results for IRF-5 protein expression. RmIL-4 stimulation decreased IRF-5 expression in control scrambled RNA transfected MO cells ($P < 0.05$), which was increased in miR-21 antagomir transfected cells ($P < 0.01$).

M2 macrophage restoration aggravates AHR, eosinophilic airway inflammation and IL-4/13 expression in miR-21 antagomir administrated mice

Fig. 8 demonstrates the changes in AHR, BALF cell counts and IL-4/13 expression by M2 macrophage inhalation in the miR-21 suppressed OVA mice. AHR increased in the M2 inhaled mice compared to the miR-21 antagomir/vehicle-treated group ($P < 0.05$). Total cell ($P < 0.001$), eosinophil counts ($P < 0.01$) and expression of Th2 cytokine IL4/13 ($P < 0.05/P < 0.01$) in BALF increased significantly in the OVA + miR-21 antagomir/M2 group compared to the miR-21 antagomir/vehicle mice.

DISCUSSION

The results of the present study showed that miR-21 KO led to significantly decreased AHR, eosinophilic airway inflammation, expression of BALF Th2 cytokine IL-4, IL-5, and IL-13,

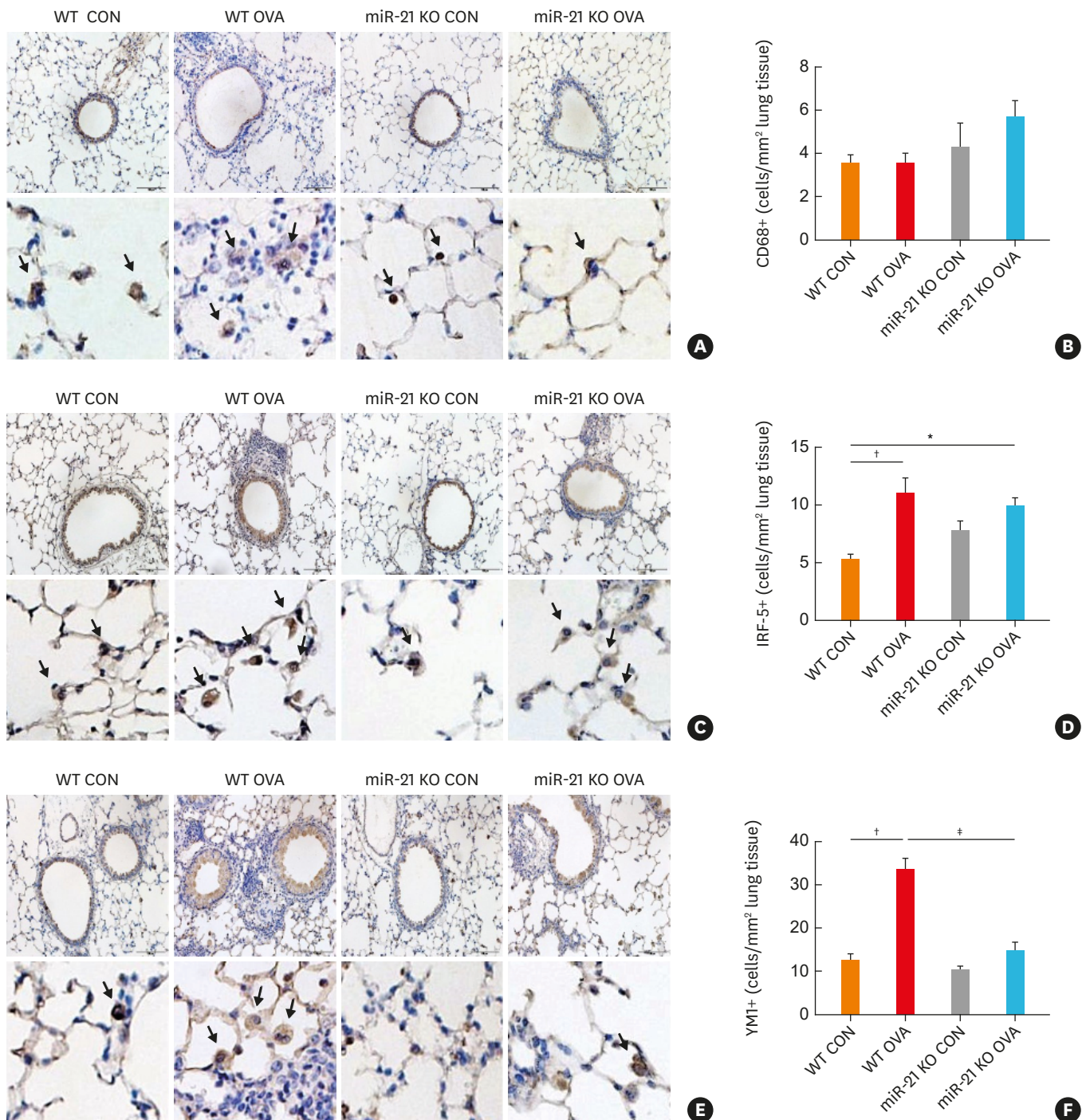


Fig. 4. Effect of miR-21 KO on immunohistochemistry stained lung tissues. Representative photomicrographs of CD68 positive total macrophages (A) in lung sections from mice of the different treatment groups are shown ($\times 200$). (B) Quantification of CD68 positive areas are expressed as the mean \pm SEM ($n = 5-8$ /group). Representative photomicrographs of (C) IRF5 and (E) YMT1 positive macrophages in lung sections from mice of the different treatment groups are shown ($\times 200$). Quantification of (D) IRF5 and (F) YMT1 positive areas are expressed as the mean \pm SEM ($n = 5-8$ /group). WT, wild type; CON, control; OVA, ovalbumin; KO, knock-out; miR-21, microRNA-21; IRF5, interferon regulatory factor 5; SEM, standard error of the mean. * $P < 0.05$, $^{\dagger}P < 0.001$ compared to the CON group; $^{\ddagger}P < 0.001$ compared to the WT OVA group.

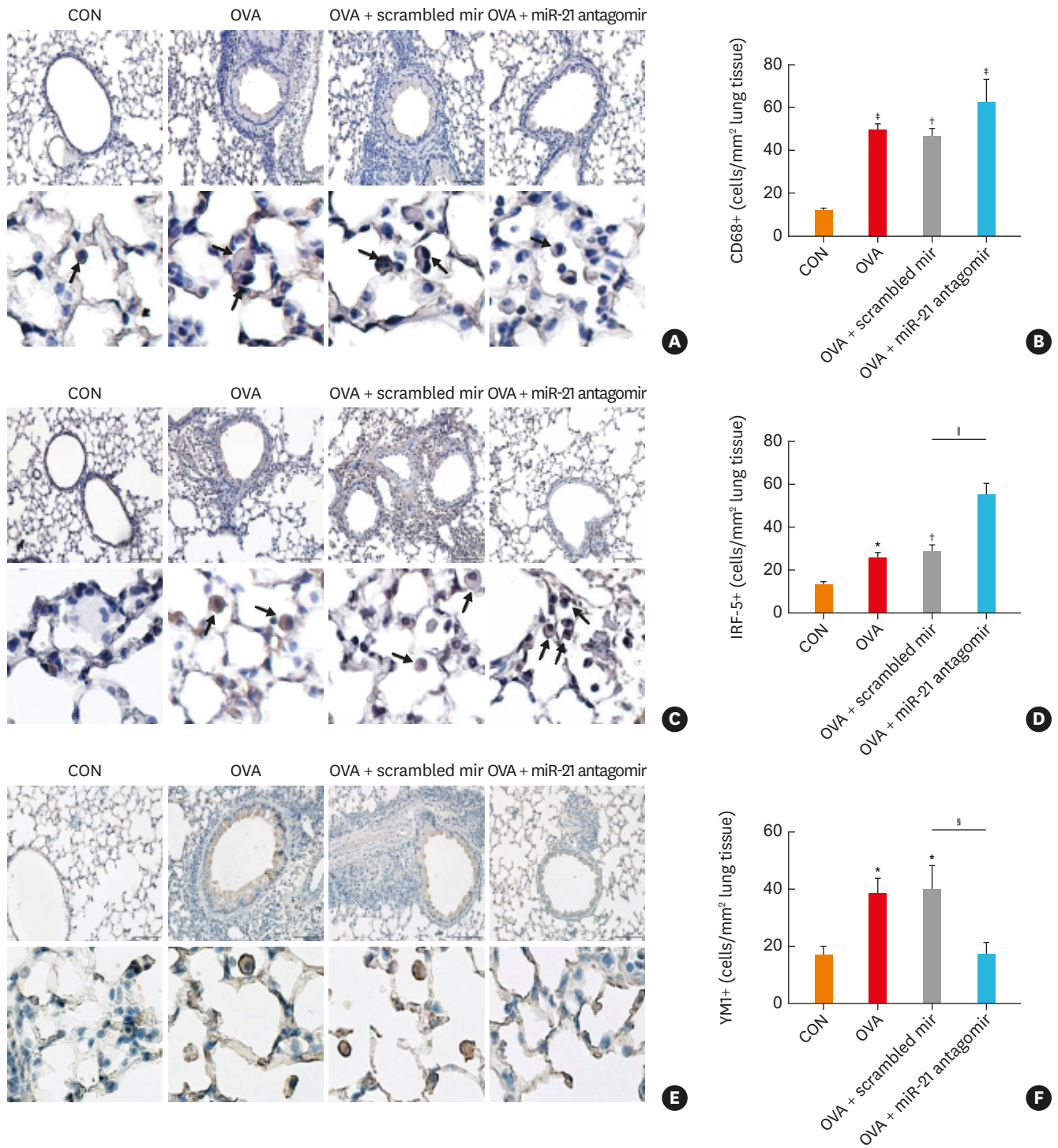


Fig. 5. Effect of anti-miR-21 antagonomir inhalation on immunohistochemistry stained lung tissues. Representative photomicrographs of CD68 positive total macrophages (A) in lung sections from mice of the different treatment groups are shown ($\times 200$). (B) Quantification of CD68 positive areas are expressed as the mean \pm SEM (n = 5–8/group). Representative photomicrographs of (C) IRF5 and (E) YM1 positive macrophages in lung sections from mice of the different treatment groups are shown ($\times 200$). Quantification of (D) IRF5 and (F) YM1 positive areas are expressed as the mean \pm SEM (n = 5–8/group). CON, control; OVA, ovalbumin; miR-21, microRNA-21; IRF5, interferon regulatory factor 5; SEM, standard error of the mean. * $P < 0.05$, † $P < 0.01$, ‡ $P < 0.001$ compared to the CON group; § $P < 0.05$, † $P < 0.001$ compared to the wild type OVA group.

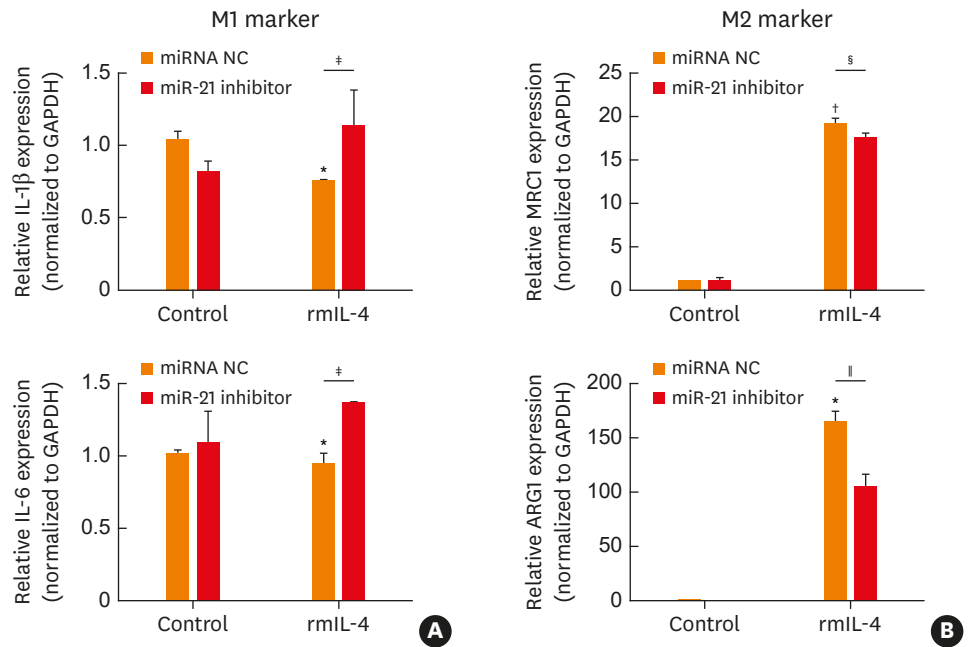


Fig. 6. Effect of anti-miR-21 antagonomir transfection on expression of M1 and M2 macrophages markers in MO macrophage (RAW 264.7) after rmIL-4 stimulation. RAW264.7 cells were transfected with anti-miR-21 antagonomir or control scrambled RNA (NC) for 72 hours and then stimulated with rmIL-4 for 18 hours. Expression of (A) M1 macrophage marker IL-1β, IL-6 and (B) M2 marker MRC1, ARG1. IL, interleukin; GAPDH, glyceraldehyde 3-phosphate dehydrogenase; miR-21, microRNA-21; rm, recombinant mouse; NC, negative control; MRC1, C-type mannose receptor 1; ARG1, arginase 1. **P* < 0.01, †*P* < 0.001 compared to the control NC cells; ‡*P* < 0.05, §*P* < 0.01, ¶*P* < 0.001 compared to the rmIL-4 stimulated NC cells.

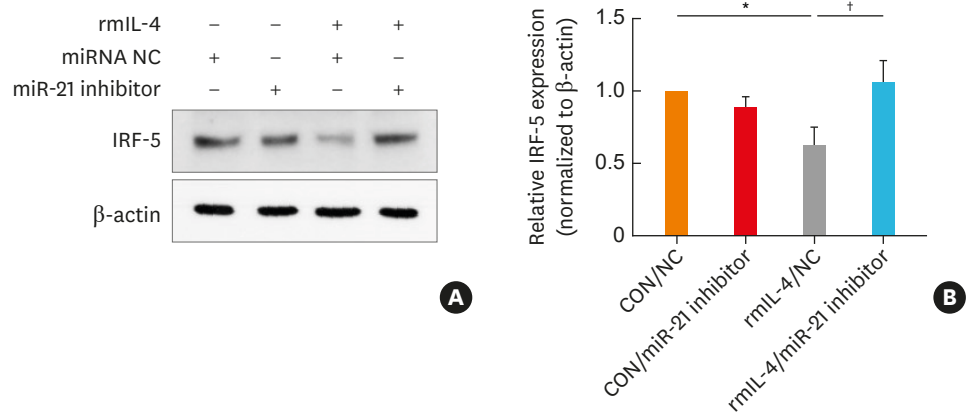


Fig. 7. Effect of anti-miR-21 antagonomir transfection on expression of IRF-5 in MO macrophage (RAW 264.7) after rmIL-4 stimulation. RAW264.7 cells were transfected with anti-miR-21 antagonomir or control scrambled RNA (NC) for 72 hours and then stimulated with rmIL-4 for 48 hours. (A) Representative immunoblot showed the expression of M1 macrophage marker IRF-5 in transfected cells. β-actin was used as a control. (B) The optical densitometry results in the different treatment groups. rm, recombinant mouse; miR-21, microRNA-21; IRF-5, interferon regulatory factor 5; NC, negative control; CON, control. **P* < 0.05, compared to the control NC cells; †*P* < 0.01 compared to the rmIL-4 stimulated NC cells.

and increased IL-12 and IFN-γ after OVA inhalation and challenge compared to WT asthma mice. Moreover, miR-21 deficiencies generated by miR-21 KO or miR-21 antagonomir inhalation decreased the expression of M2 alveolar macrophage. MiR-21 KO asthma mice exhibited

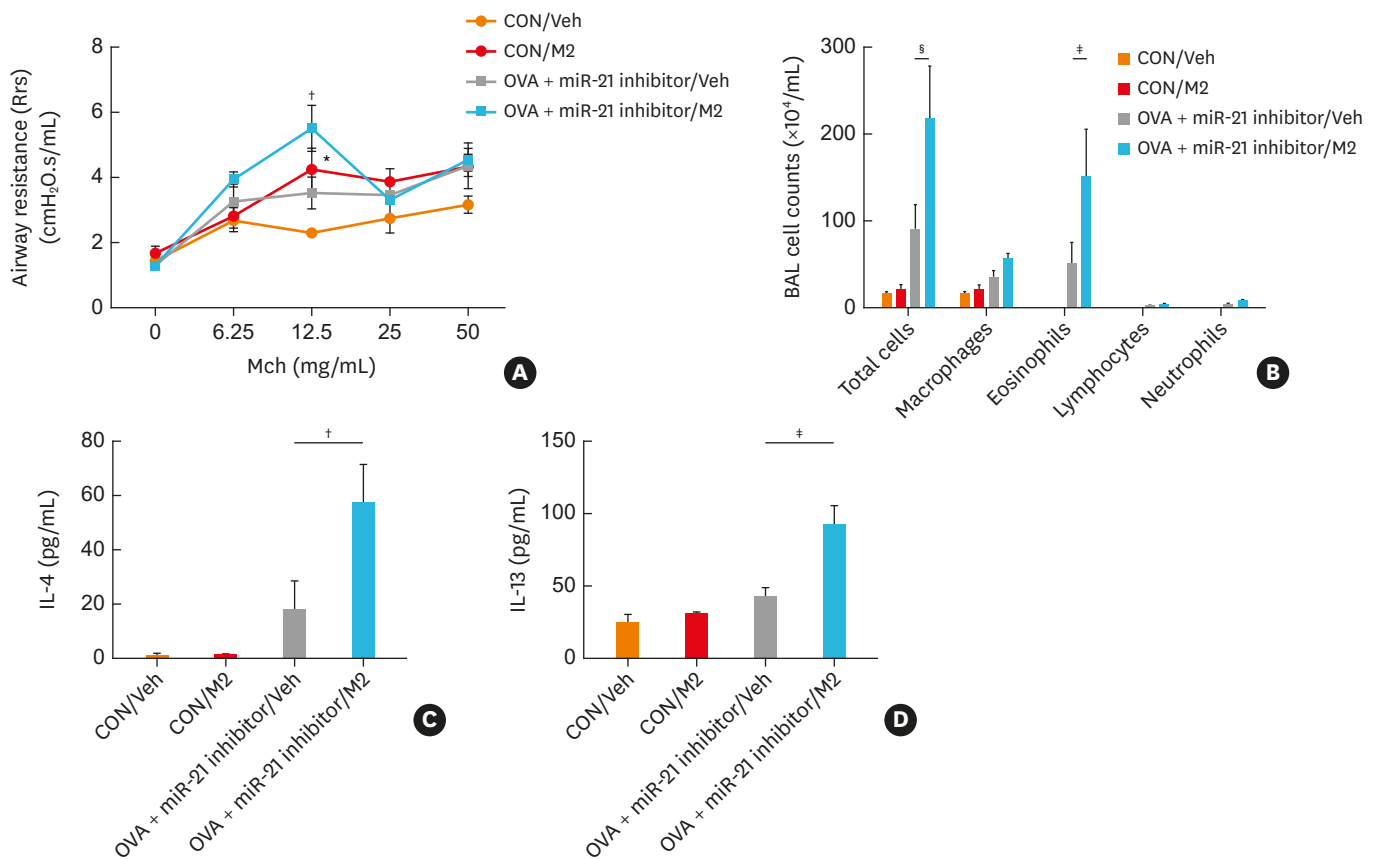


Fig. 8. Effect of M2 macrophage restoration in anti-miR-21 antagonist inhaled OVA mice. M2 macrophages were isolated from OVA mice lung and intranasally administered in anti-miR-21 antagonist inhaled asthmic mice at the day of last OVA challenge. Changes of AHR (A), BALF total cell and percentages of differential cell counts (B) were analyzed. Expression of IL-4 (C) and IL-13 (D) in BALF were measured by enzyme-linked immunosorbent assay. The values are expressed as the mean ± standard error of the mean (n = 5/group).

Rrs, respiratory system resistance; Mch, methacholine; CON, control; Veh, vehicle; OVA, ovalbumin; BAL, bronchoalveolar lavage; BALF, bronchoalveolar lavage fluid; IL, interleukin.

*P < 0.05 compared to the CON/Veh group; †P < 0.05, ‡P < 0.01, §P < 0.001 compared to OVA + miR-21 antagonist/vehicle group.

decreased airway inflammation and goblet cell hyperplasia in the lung tissues. Transfection of M0 macrophages with anti-miR-21 antagonist increased M1 macrophage markers (IRF-5, IL-1 β , and IL-6) and decreased M2 markers (MRC1 and ARG1) upon IL-4 stimulation. Moreover, restoration of M2 macrophages isolated from OVA mice increased AHR, airway eosinophilic inflammation and BALF IL-4/13 expressions in miR-21 antagonist-treated asthmatic mice. These results demonstrated the role of miR-21 in the mouse lung with an effect not only on the polarization of M2 macrophages but also on eosinophilic airway inflammation, AHR, and airway remodeling process.

Generally, blood monocytes are recruited into the tissue from where they differentiate into macrophages or dendritic cells.^{20,21} The polarization of macrophages into M1 or M2 macrophages depends on the microenvironments.⁷ Classic activation (M1) transforms macrophages into antimicrobial effector cells, upon stimulation by cytokine IFN- γ , bacterial lipopolysaccharide (LPS), and granulocyte macrophage-colony stimulation factor (GM-CSF).²² IFN- γ and GM-CSF recruit Janus kinase 1 (Jak1) and Jak2 adaptors, which activate IRFs. LPS mediates toll-like receptor (TLR) 4 cascade under the control of nuclear factor kappa-light chain-enhancer of activated B cells, activator protein 1, IRFs and the STAT 1. TLR4 activation

leads to the signaling of the pro-inflammatory cytokine, IL-1 β , IL-6, IL-12, and IFN- β .²² Alternative (M2) polarization is known to be associated with a high level of IL-10 and IL-1 receptor antagonist and a low level of IL-12. The signature of M2 macrophage is the production of the ARG1 enzyme that depletes L-arginase, leading to suppression of T-cell response.²³

Airway inflammation in bronchial asthma has been characterized to involve various kinds of cells such as eosinophils, neutrophils, lymphocytes, and macrophages. Phenotyping of the patients based on eosinophils or neutrophils is clinically important to guide pharmacological therapy; however, the most abundant cells present in the asthmatic airway are macrophages and monocytes.³ Gundra *et al.*²⁴ reported that alternatively activated (M2) macrophages are derived from both blood monocytes and tissue macrophages, and they have distinct transcription profiles and phenotypes. In their study results, monocyte-derived alternatively activated macrophages were identified to be more involved in immune regulation.²⁴ In our study, we initially checked the changes in airway macrophages based on BALF differential count and then in lung tissues by IHC stain. It can be seen in **Fig. 2** that BALF macrophage cell counts seem to be slightly elevated in the OVA mice compared to the control mice in both WT and miR-21 KO groups. However, there were no statistically significant differences in elevation of total macrophages in the OVA mice compared to the control mice and decrease in the miR-21 KO OVA mice compared to the WT OVA mice. It is clear in **Fig. 6** that the elevation of CD68 (+) total macrophages in the OVA mice exhibited no statistical significance compared to the WT miR-21 KO control group. However, counts of M2 macrophages were significantly suppressed both in the miR-21 KO OVA mice and the anti-miR-21 antagomir-treated OVA mice compared to the miR-21 WT OVA and the scrambled-RNA-treated OVA mice (**Figs. 4 and 5**).

We used miR-21 KO mice and administered anti-miR-21 antagomir from the day of OVA sensitization. In accordance with the published results and our data, we assumed that miR-21 suppression probably affects the polarization of immature monocytes to M2 macrophages during asthmatic airway inflammation. *In vitro* study results on the transfection of M0 macrophages with miR-21 antagomir also supported our hypothesis. Transcription of M1 and M2 macrophages markers after rmIL-4 stimulation showed an increased level of M1 markers (IL-1 β , IL-6, and IRF5) and decreased level of M2 markers (MRC1 and ARG1) in the miR-21 antagomir-transfected cells. IRF5 is a well-known M1 macrophage marker and is proposed as a transcription regulator which directly activates transcription of genes encoding IL-12 subunit and represses the genes encoding IL-10.²⁵ There was a report that miR-22-3p modulated M2 macrophage polarization via IRF5 in a spinal cord ischemia/reperfusion injury rat model.²⁶ Although further studies are needed, IRF5 might be a target of miR-21, and up-regulation of IRF5 by miR-21 antagomir transfection could have affected the macrophage polarization.

Inhibition of M2 macrophage polarization in mouse asthma models has been evaluated in the previous studies with cynaropicrin, a galectin-3 pathway inhibitor,^{27,28} and IL-4 receptor α (IL-4R α)-deficient mice.²⁹ Suppression of M2 macrophages with cynaropicrin treatment during induction of airway allergic inflammation by house dust mites generated less severe eosinophilic lung inflammation and collagen deposition, which was different from cynaropicrin treatment after induction of allergic inflammation. Interestingly, airway neutrophilic inflammation and AHR were worse in mice treated with cynaropicrin as compared to control mice. This experiment showed the dual role of M2 macrophages in the development of eosinophilic inflammation, prevention of neutrophilic airway inflammation, and worsening AHR. Our study results demonstrated partial agreement with those of a study conducted

by Draijer *et al.*²⁷ The decrease in airway eosinophilic inflammation by miR-21 KO or miR-21 antagonist inhalation was a consistent finding; however, a decrease in AHR and goblet cell hyperplasia by miR-21 deficiency was contradictory from M2 inhibition by cynaropicrin. Until now, the role of miR-21 in allergic airway inflammation was known to inhibit IL-12/IFN- γ pathway and Th1 polarization.^{9,13} Although we did not examine Th1/Th2 polarization in this study, it was apparent that miR-21 suppression by KO significantly suppressed BALF IL-4, IL-5, IL-10, and IL-13 expressions as well as increased the expression of IL-12 and IFN- γ . We assumed that the interactions between decreased M2 macrophage polarization and Th2 cells in lung tissues in miR-21 deficiency might have influenced airway eosinophils and remodeling processes during development of OVA-induced asthmatic airway inflammation.

This hypothesis could be reinforced with other experimental results, which made airway inflammation in mice with genetically abrogated IL-4R α . Deletion of IL-4R α in mature alveolar, interstitial, and CD11b⁺MHCII⁺ macrophages failed to suppress eosinophilic airway inflammation, AHR, mucus secretion, and collagen deposition.²⁹ M2 macrophages that newly polarize from immature macrophages or recruited monocytes from blood might play more crucial roles than mature tissue macrophages in the development of airway eosinophilic inflammation, AHR, and remodeling. Our study results are unique in terms of defining the role of miR-21 in alternative (M2) macrophage polarization based on both *in vivo* and *in vitro* studies. Moreover, decreased AHR and goblet cell hyperplasia by suppressed M2 macrophages through miR-21 deficiency were intriguing aspects to be considered.

Until now, studies about the role of M2 macrophages in terms of the inflammatory or adaptive immune pathway are sufficient; however, there are still debates on the development of airway remodeling and the severity of asthma.²⁷ In human bronchial biopsy specimens, alternatively activated macrophage counts exhibited a positive correlation with peak expiratory flow variation, which reflects AHR.⁶ On the contrary, the marker of M1 macrophage, IRF5 had a higher expression level in BALF of severe asthmatics compared to mild ones.³⁰ This study also demonstrated that IRF5^{-/-} mice with severe asthma showed higher Th2 response, lower IFN- γ , and IL-17 responses with restored corticosteroid responses.³⁰ Another study using a potential inhibitor of M2 macrophage serum amyloid P (SAP) described that SAP treatment decreased AHR, mucus cell hyperplasia, and collagen deposition in an asthma mouse model.³¹ Based on the previously reported findings and results of Nieuwenhuizen's IL-4R-deficient mice²⁹ and Draijer's cynaropicrin treated mice,²⁷ it is hypothesized that the effects of M2 macrophage suppression on the airway remodeling process should depend on the timing and mechanism of inhibiting M2 macrophage polarization.

There are some limitations to our study. Analysis of airway macrophage polarization would have been better performed with BALF in mice as well as lung tissues. We measured counts of M1/M2 macrophages in the lung tissues after BAL and expression of Th1/Th2 cytokines in BALF instead of the percentage of macrophages and Th1/Th2 cells. It is believed that examination of airway macrophage polarization and T cells with BALF might provide a more comprehensive understanding of the interactions between miR-21-deficient macrophages and T cells during allergic airway inflammation in miR-21 KO mice.

In conclusion, the miR-21 deficiency was effective in decreasing airway eosinophilic inflammation, AHR, and airway remodeling in the OVA-induced asthma mice model. The mechanism of decreased airway remodeling in the miR-21 KO mice could be attributed to the suppressed alternative (M2) polarization of pulmonary macrophages and the interactions

between M2 macrophages and Th2 cells. Since inhibition of M2 macrophage polarization had positive effects on relieving eosinophilic airway inflammation, AHR and airway remodeling, miR-21 antagonism is proposed as a new therapeutic approach targeting M2 macrophages.

ACKNOWLEDGMENTS

This study was supported by a grant from the Research Foundation of Physician, The Catholic University of Korea and the Bio & Medical Technology Development Program of the National Research Foundation (NRF) funded by the Korean government (MSIT) (No. 5-2020-A0154-00021).

SUPPLEMENTARY MATERIAL

Supplementary Fig. S1

Replacement of M2 macrophages in mice administered with a miR-21 inhibitor. M2 macrophages were isolated from OVA mice lung by fluorescence-activated cell sorting with anti-CD45, anti-F4/80 and anti-CD206 antibodies (A). Experimental schedule of M2 macrophage replacement into anti-miR-21 inhibitor administrated OVA asthma mice (B).

[Click here to view](#)

REFERENCES

1. Gon Y, Hashimoto S. Role of airway epithelial barrier dysfunction in pathogenesis of asthma. *Allergol Int* 2018;67:12-7.
[PUBMED](#) | [CROSSREF](#)
2. Park SC, Kim H, Bak Y, Shim D, Kwon KW, Kim CH, et al. An alternative dendritic cell-induced murine model of asthma exhibiting a robust Th2/Th17-skewed response. *Allergy Asthma Immunol Res* 2020;12:537-55.
[PUBMED](#) | [CROSSREF](#)
3. Fricker M, Gibson PG. Macrophage dysfunction in the pathogenesis and treatment of asthma. *Eur Respir J* 2017;50:1700196.
[PUBMED](#) | [CROSSREF](#)
4. Sica A, Mantovani A. Macrophage plasticity and polarization: *in vivo* veritas. *J Clin Invest* 2012;122:787-95.
[PUBMED](#) | [CROSSREF](#)
5. Girodet PO, Nguyen D, Mancini JD, Hundal M, Zhou X, Israel E, et al. Alternative macrophage activation is increased in asthma. *Am J Respir Cell Mol Biol* 2016;55:467-75.
[PUBMED](#) | [CROSSREF](#)
6. Melgert BN, ten Hacken NH, Rutgers B, Timens W, Postma DS, Hylkema MN. More alternative activation of macrophages in lungs of asthmatic patients. *J Allergy Clin Immunol* 2011;127:831-3.
[PUBMED](#) | [CROSSREF](#)
7. Lawrence T, Natoli G. Transcriptional regulation of macrophage polarization: enabling diversity with identity. *Nat Rev Immunol* 2011;11:750-61.
[PUBMED](#) | [CROSSREF](#)
8. Wang Z, Ji N, Chen Z, Sun Z, Wu C, Yu W, et al. MiR-1165-3p suppresses Th2 differentiation via targeting IL-13 and PPM1A in a mouse model of allergic airway inflammation. *Allergy Asthma Immunol Res* 2020;12:859-76.
[PUBMED](#) | [CROSSREF](#)
9. Lu TX, Munitz A, Rothenberg ME. MicroRNA-21 is up-regulated in allergic airway inflammation and regulates IL-12p35 expression. *J Immunol* 2009;182:4994-5002.
[PUBMED](#) | [CROSSREF](#)

10. Sawant DV, Yao W, Wright Z, Sawyers C, Tepper RS, Gupta SK, et al. Serum microRNA-21 as a biomarker for allergic inflammatory disease in children. *MicroRNA* 2015;4:36-40.
[PUBMED](#) | [CROSSREF](#)
11. Taka S, Tzani-Tzanopoulou P, Wanstall H, Papadopoulos NG. MicroRNAs in asthma and respiratory infections: identifying common pathways. *Allergy Asthma Immunol Res* 2020;12:4-23.
[PUBMED](#) | [CROSSREF](#)
12. Wardzyńska A, Pawelczyk M, Rywaniak J, Kurowski M, Makowska JS, Kowalski ML. Circulating microRNAs and T-cell cytokine expression are associated with the characteristics of asthma exacerbation. *Allergy Asthma Immunol Res* 2020;12:125-36.
[PUBMED](#) | [CROSSREF](#)
13. Lu TX, Hartner J, Lim EJ, Fabry V, Mingler MK, Cole ET, et al. MicroRNA-21 limits *in vivo* immune response-mediated activation of the IL-12/IFN-gamma pathway, Th1 polarization, and the severity of delayed-type hypersensitivity. *J Immunol* 2011;187:3362-73.
[PUBMED](#) | [CROSSREF](#)
14. Lee HY, Lee HY, Choi JY, Hur J, Kim IK, Kim YK, et al. Inhibition of microRNA-21 by an antagomir ameliorates allergic inflammation in a mouse model of asthma. *Exp Lung Res* 2017;43:109-19.
[PUBMED](#) | [CROSSREF](#)
15. Coyle AJ, Lloyd C, Tian J, Nguyen T, Eriksson C, Wang L, et al. Crucial role of the interleukin 1 receptor family member T1/ST2 in T helper cell type 2-mediated lung mucosal immune responses. *J Exp Med* 1999;190:895-902.
[PUBMED](#) | [CROSSREF](#)
16. Tarkowski M, Vanoirbeek JA, Vanhooren HM, De Vooght V, Mercier CM, Ceuppens J, et al. Immunological determinants of ventilatory changes induced in mice by dermal sensitization and respiratory challenge with toluene diisocyanate. *Am J Physiol Lung Cell Mol Physiol* 2007;292:L207-14.
[PUBMED](#) | [CROSSREF](#)
17. Mabalirajan U, Dinda AK, Kumar S, Roshan R, Gupta P, Sharma SK, et al. Mitochondrial structural changes and dysfunction are associated with experimental allergic asthma. *J Immunol* 2008;181:3540-8.
[PUBMED](#) | [CROSSREF](#)
18. Padrid P, Snook S, Finucane T, Shiue P, Cozzi P, Solway J, et al. Persistent airway hyperresponsiveness and histologic alterations after chronic antigen challenge in cats. *Am J Respir Crit Care Med* 1995;151:184-93.
[PUBMED](#) | [CROSSREF](#)
19. Rhee CK, Kim JW, Park CK, Kim JS, Kang JY, Kim SJ, et al. Effect of imatinib on airway smooth muscle thickening in a murine model of chronic asthma. *Int Arch Allergy Immunol* 2011;155:243-51.
[PUBMED](#) | [CROSSREF](#)
20. Zaslona Z, Przybranowski S, Wilke C, van Rooijen N, Teitz-Tennenbaum S, Osterholzer JJ, et al. Resident alveolar macrophages suppress, whereas recruited monocytes promote, allergic lung inflammation in murine models of asthma. *J Immunol* 2014;193:4245-53.
[PUBMED](#) | [CROSSREF](#)
21. Wynn TA, Chawla A, Pollard JW. Macrophage biology in development, homeostasis and disease. *Nature* 2013;496:445-55.
[PUBMED](#) | [CROSSREF](#)
22. Essandoh K, Li Y, Huo J, Fan GC. MiRNA-mediated macrophage polarization and its potential role in the regulation of inflammatory response. *Shock* 2016;46:122-31.
[PUBMED](#) | [CROSSREF](#)
23. Hao NB, Lü MH, Fan YH, Cao YL, Zhang ZR, Yang SM. Macrophages in tumor microenvironments and the progression of tumors. *Clin Dev Immunol* 2012;2012:948098.
[PUBMED](#) | [CROSSREF](#)
24. Gundra UM, Girgis NM, Ruckerl D, Jenkins S, Ward LN, Kurtz ZD, et al. Alternatively activated macrophages derived from monocytes and tissue macrophages are phenotypically and functionally distinct. *Blood* 2014;123:e110-22.
[PUBMED](#) | [CROSSREF](#)
25. Krausgruber T, Blazek K, Smallie T, Alzabin S, Lockstone H, Sahgal N, et al. IRF5 promotes inflammatory macrophage polarization and TH1-TH17 responses. *Nat Immunol* 2011;12:231-8.
[PUBMED](#) | [CROSSREF](#)
26. Fang H, Yang M, Pan Q, Jin HL, Li HF, Wang RR, et al. MicroRNA-22-3p alleviates spinal cord ischemia/reperfusion injury by modulating M2 macrophage polarization via IRF5. *J Neurochem*. Forthcoming 2020.
[PUBMED](#) | [CROSSREF](#)
27. Draijer C, Robbe P, Boorsma CE, Hylkema MN, Melgert BN. Dual role of YM1+ M2 macrophages in allergic lung inflammation. *Sci Rep* 2018;8:5105.
[PUBMED](#) | [CROSSREF](#)

28. MacKinnon AC, Farnworth SL, Hodgkinson PS, Henderson NC, Atkinson KM, Leffler H, et al. Regulation of alternative macrophage activation by galectin-3. *J Immunol* 2008;180:2650-8.
[PUBMED](#) | [CROSSREF](#)
29. Nieuwenhuizen NE, Kirstein F, Jayakumar J, Emedi B, Hurdayal R, Horsnell WGC, et al. Allergic airway disease is unaffected by the absence of IL-4R α -dependent alternatively activated macrophages. *J Allergy Clin Immunol* 2012;130:743-750.e8.
[PUBMED](#) | [CROSSREF](#)
30. Oriss TB, Raundhal M, Morse C, Huff RE, Das S, Hannum R, et al. IRF5 distinguishes severe asthma in humans and drives Th1 phenotype and airway hyperreactivity in mice. *JCI Insight* 2017;2:e91019.
[PUBMED](#) | [CROSSREF](#)
31. Moreira AP, Cavassani KA, Hullinger R, Rosada RS, Fong DJ, Murray L, et al. Serum amyloid P attenuates M2 macrophage activation and protects against fungal spore-induced allergic airway disease. *J Allergy Clin Immunol* 2010;126:712-721.e7.
[PUBMED](#) | [CROSSREF](#)